

## Multiple Quantum Transitions Induced by Irradiating Single Quantum Coherence in a Heteronuclear Spin System

Bang-Chih Jiang ( 蔣邦智 ), Xijia Miao<sup>a</sup> ( 繆希茹 ),  
Lian-Pin Hwang\* ( 黃良平 ) and Chaohui Ye<sup>b</sup> ( 葉朝輝 )

*Institute of Atomic and Molecular Science, Academia Sinica, and Department of Chemistry,  
National Taiwan University, Taipei, Taiwan, R.O.C.*

In a heteronuclear spin system, with initially prepared single quantum (SQ) coherence of X-spin, the irradiation of the proton spins will induce all the possible transitions including those SQs and multiple quanta (MQs) available in the system to be studied. The MQs appear in a rather weak irradiation while a strong irradiation results in a complete decoupling situation. Theoretical analysis is made to explain this phenomenon and is agreed qualitatively with experiments in the CH<sub>2</sub> group. This phenomenon of MQ induction may happen in a decoupling experiment when the effective irradiation strength is rather weak and it may also provide a convenient approach to create and then to manipulate MQ coherences in heteronuclear spin systems.

### INTRODUCTION

It is well known that multiple quantum (MQ) NMR has extended the applicability of NMR spectroscopy.<sup>1-3</sup> However, appearance of undesirable or unexpected MQ signals in experimental spectra is sometimes confusing. Here in this paper we will report the observation of MQ signals which are induced by irradiating single quantum coherences previously manipulated in the experiment in heteronuclear spin system. The irradiation strength, hereafter we denote as  $\omega_1$ , is much weaker than the one when complete decoupling occurs. This phenomenon, to our knowledge, has long been ignored.

Correction of decoupled NMR spectrum is usually a routine measurement for heteronuclear spin systems. The decoupling efficiency depends upon both the r.f. field strength of decoupling irradiation and its frequency offset to the Larmor frequency of decoupled spins. Generally, the effective strength of decoupling irradiation decreases with increasing offset when the irradiation  $\omega_1$  is given. The decoupling course with an increasingly effective field has been clearly demonstrated in the early NMR studies.<sup>4,5</sup> However, there has been no report on how a coherent spin state previously prepared responds to an irradiation at the decoupling channel.

### EXPERIMENTAL SECTION

The experimental schemes are shown in Fig. 1. The

experimental course has been divided into two periods: preparation and detection. During the preparation period a desirable coherent state of the heteronuclear spin system is manipulated by inserting a proper pulse sequence with phase cycling. During the detection period, a continuous irradiation is employed at the decoupling channel while observing the NMR signals of the X-nuclei. The experimental schemes are basically the same as in Raman magnetic resonance experiments for the heteronuclear spin systems.<sup>6-8</sup> These schemes are also readily adapted to those double resonance experiments<sup>9</sup> in which the irradiation frequency is turned on at or close to one of the resonant frequencies of the decoupled spins. When the irradiation is weak in comparison with the case when complete spin decoupling appears, a prepared single quantum coherence of X-spin will induce MQ transitions by the heteronuclear frequency irradiation. Understanding this phenomenon can therefore enhance our knowledge of decoupling experiments as well as Raman magnetic resonance experiments of heteronuclear spin systems.

We have chosen the methylene group in Dichloromethane (E. Merck) as a heteronuclear spin system of AX<sub>2</sub>. The NMR spectra were measured on a Bruker ARX-500 spectrometer whose proton and carbon frequencies are ca. 500 and 125 MHz, respectively. All the measurements were conducted at room temperature.

The experiment in scheme (a) is similar to a routine <sup>13</sup>C NMR measurement with a wide range of proton decoupling irradiation. The INEPT pulse sequence<sup>10</sup> has been inserted in the preparation period in scheme (b), then the <sup>13</sup>C

a. Present address: Department of Chemistry, University of Cambridge, Lensfield Road, CB2 1EW, UK.

b. On sabbatical leave from Wuhan Institute of Physics, Chinese Academy of Science, Wuhan 430071, China.

NMR signals were measured during the detection period with various irradiation strength at the proton resonant frequency.

We denote the nuclear spin of  $^{13}\text{C}$  as  $S$ , while the proton spin as  $I$ . At the end of the preparation period, the manipulated coherent states can be expressed by spin operators as  $S_x$  in scheme (a) and  $2I_zS_x$  in scheme (b), respectively. Both  $S_x$  and  $2I_zS_x$  are single quantum coherences which induce the traditional  $^{13}\text{C}$  NMR spectra without irradiation during the detection period, i.e., the proton coupled spectra in Fig. 2a for scheme (a) and in Fig. 3a for scheme (b). As we can see in these spectra, the normal binomial intensity ratio 1:2:1 for Fig. 2a and the INEPT intensity ratio -1:0:1 for Fig. 3a has been respectively obtained both with a  $J$ -coupling constant of 187 Hz for the methylene group.

In Figs. 2 and 3, we show also the spectra for the weak(b), medium(c), and strong(d) irradiation cases, where the irradiation strengths  $\omega_1$  are 45, 450, and 4500 Hz, re-

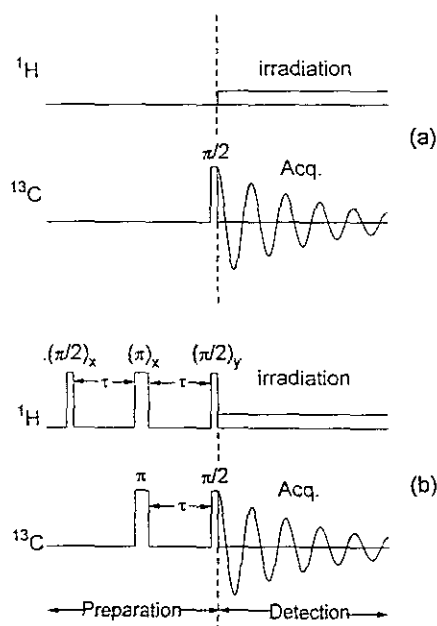


Fig. 1. Experimental schemes. The experiment can be divided into two periods: preparation and detection. In scheme (a), a single quantum SQ coherence of the spin system, i.e.,  $S_x$ , is created during the preparation period. This SQ coherence is irradiated by an r.f. field at the proton frequency while acquiring carbon signals during the detection period. The irradiation field strength  $\omega_1$  is variable in the experiments. In scheme (b), an INEPT pulse sequence is inserted into the preparation period. Therefore a SQ coherence, i.e.,  $2I_zS_x$ , can be created at the end of this period. The experimental procedures in schemes (a) and (b) are the same during the detection period.

spectively. There was no observation offset for the  $^{13}\text{C}$  spectra while the irradiation offset was 100 Hz for the proton Larmor frequency in all the experiments.

Fig. 2b shows the  $^{13}\text{C}$  spectrum when the irradiation was rather weak. A total of seven multiple quantum transitions now appear besides the two single quantum transitions. We can assign these nine transitions according to their position relationship with the multiple quantum orders. By numbering these transitions from 1 as the one on the far

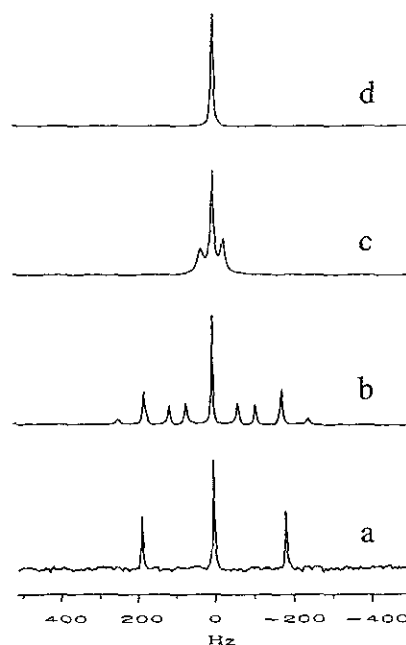


Fig. 2. Experimental  $^{13}\text{C}$  NMR spectra of Dichloromethane in scheme (a). The irradiation offset is 100 Hz. The initial coherent state at the beginning of detection period is  $S_x$ . The central peaks of the following traces are normalized to the same intensity. a.  $\omega_1 = 0$ , this is a proton coupled  $^{13}\text{C}$  spectrum. Coupling constant of this  $\text{CH}_2$  group thus can be obtained as 187 Hz. b.  $\omega_1 = 45$  Hz. The  $^{13}\text{C}$  spectrum shows all the possible transitions in the system. We have numbered the resonances from the left side to the right sequentially, and the MQs can also be expressed in raising and lowering operators: 1 — Triple Quantum (3Q),  $S^{\pm 3}I^{\pm 3}$ ; 2, 8 — outside single quantum (SQ); The noticeable shift of these two resonances in comparison with the positions in a is due to the irradiation. 3, 4 — double quantum (DQ);  $S^{\pm 2}I^{\pm 2}$  and  $S^{\pm 2}I^{\pm 2}$ ; 5 — central single quantum; 6, 7 — zero-quantum (ZQ),  $S^{\pm 1}I^{\pm 1}$  and  $S^{\pm 1}I^{\pm 1}$ . c.  $\omega_1 = 450$  Hz. The two outside SQs come much closer in medium irradiation. The residual splittings indicate an incomplete decoupling case. d.  $\omega_1 = 4500$  Hz. The three SQs have merged together indicating a complete decoupling case. The actual intensity is twice as shown here.

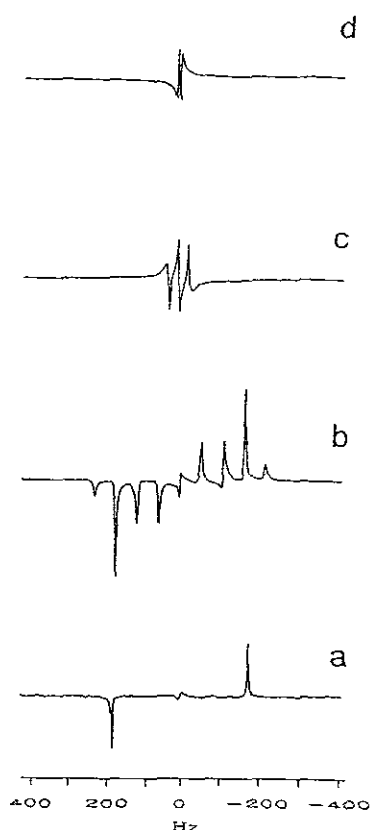


Fig. 3. Experimental  $^{13}\text{C}$  NMR spectra of Dichloromethane in scheme (b). Here the coherent state at the beginning of detection period is  $2I_zS_x$ . The irradiation offset is 100 Hz throughout the experiment. a.  $\omega_1 = 0$ . The  $^{13}\text{C}$  spectrum shows a typical INEPT pattern of the  $\text{CH}_2$  group. The two reversed outside single transitions and the suppressed central SQ transition results in an intensity ratio: -1:0:1. However, the central SQ transition is not suppressed completely, and a weak differential signal can still be seen in the center of the spectrum. b.  $\omega_1 = 45$  Hz. The  $^{13}\text{C}$  spectrum shows all the possible transitions including SQs and MQs in the  $\text{CH}_2$  group. In comparison with the spectrum in Fig. 2b, all the signals in the positive frequency side are inverted due to the influence of proton magnetization  $I_z$  existing in the initial coherent state. Besides, the central SQ signal, which has been greatly suppressed, remains a differential residual signal in the middle of the spectrum. c.  $\omega_1 = 450$  Hz. The incomplete proton decoupled  $^{13}\text{C}$  spectrum. The spectrum is somehow distorted because the two outside SQ signals interfere and there is incomplete suppression of the central SQ signal. d.  $\omega_1 = 4500$  Hz. The complete proton decoupled  $^{13}\text{C}$  spectrum. The residual signal is due to incomplete suppression of the central SQ in the  $\text{CH}_2$  system by INEPT sequence.

left to 9 on the far right in Fig. 2b, we assign them as 1—triple quantum (3Q), 2 and 8—the outside single quantum (SQ), 5—the center SQ, 3 and 4—double quantum (DQ), 6 and 7—zero quantum (ZQ), and finally 9—forbidden single quantum (F1Q). Fig. 2c shows that when  $\omega_1$  of medium strength, i.e., 450 Hz, decoupling is not complete, i.e., a residual ca. 35 Hz splitting remains between the outside and the central SQs. However, those MQs shown in Fig. 2b have disappeared in the spectrum. Fig. 2d shows that in strong irradiation the carbons are completely decoupled with the protons. Therefore the three SQs are merged into a single peak.

Fig. 3b shows the  $^{13}\text{C}$  spectrum when the irradiation is rather weak, i.e. when  $\omega_1 = 45$  Hz for scheme(b). Since the initial coherent state created by the INEPT pulse sequence is  $2I_zS_x$ , the signals in the positive frequency side show negative intensities while the central SQ has the shape of a differential curve with a small intensity. The central SQ should have zero intensity in the INEPT spectrum. However, a residual remains due to the linewidth effect. For an intermediate irradiation strength, Fig. 3c, the two outside SQs come closer to create a differential peak between them. The two peaks are not completely canceled in intensity, Fig. 3d, when irradiation is strong.

In the above experiments we have demonstrated that a SQ coherence can induce all the possible transitions including SQs and MQs available in the spin system. The possible MQs expressed in terms of raising and lowering operators in the  $\text{CH}_2$  group are: 3Q,  $S^+I_1^+I_2^+$ ; F1Q,  $S^+I_1^+I_2^-$ ; DQ,  $S^+I_1^+$  and  $S^+I_2^+$ ; ZQ,  $S^+I_1^+$  and  $S^+I_2^+$ . All the MQ signals can be observed in a certain range of irradiation strength.

It is well known in early CW NMR<sup>11,12</sup> work that MQ transitions appear when the excitation irradiation is relatively strong so that high order perturbation effects can be manifested in the spin system. However, in those MQ work, the spin systems studied were usually homonuclear systems. Our experiments were with a heteronuclear system, i.e., observing at the  $^{13}\text{C}$  nuclear frequency while irradiating at the proton frequency. No signal will be observed if an initial coherent state was not manipulated during the preparation period. The mechanism to be concerned here in our experiments is new. In the next section we will present a theoretical analysis of this phenomenon.

### Theoretical Analysis

During the detection period, an r.f. irradiation, whose frequency is near the Larmor frequency of spin-1, is applied along the X-axis in the laboratory frame. Therefore, the total Hamiltonian of the  $\text{AX}_2$  system in the double rotating

frame during the detection period is written as

$$H = H_0 + H_1, \quad (1)$$

where

$$H_0 = \delta_s S_z + \delta I_z + JS_z I_x, \quad (2)$$

$$H_1 = \omega_1 I_x. \quad (3)$$

In Eq. (2),  $\delta_s$  is the observation offset of S-spin and was set to be zero in our experiments. Therefore the first term in Eq. 2 can be dropped.  $\delta$  is the irradiation offset,  $J$  is the spin coupling constant,  $\omega_1$  is the r.f irradiation strength. Since there are two proton spins, the spin operator  $I$  should be the sum of the two spin operators  $I_1$  and  $I_2$ . Therefore, we have

$$I_i = I_{1i} + I_{2i}, \quad i = x, y, z. \quad (4)$$

The signals of a given coherent state of the spin system can then be written as

$$\langle S_z \rangle = \text{Tr}[S_z R(t) \rho(0) R(t)^{-1}], \quad (5)$$

where  $\rho(0)$  is the density matrix of a given coherent state, e.g.,  $S_x$  and  $2I_z S_x$  in schemes (a) and (b) of our experiments, respectively.  $R(t)$  is the propagator,

$$R(t) = \exp(-iHt). \quad (6)$$

It has been shown<sup>13</sup> that for  $AX_n$  systems, their propagator can be written as

$$R(t) = \exp(-i\alpha_1 I_y) \cdot \exp(-i\alpha_2 S_z I_y) \cdot \exp(-i\delta' I_x t) \cdot \exp(-iJ S_z I_x t) \cdot \exp(i\alpha_2 S_z I_y) \cdot \exp(i\alpha_1 I_y) \quad (7)$$

where

$$J' = J \cos \alpha_1 \cos \alpha_2 + 2\omega_1 \cos \alpha_1 \sin \alpha_2 - 2\delta \sin \alpha_1 \sin \alpha_2, \quad (8)$$

$$\delta' = \delta \cos \alpha_1 \cos \alpha_2 + \omega_1 \sin \alpha_1 \cos \alpha_2 - \frac{1}{2} J \sin \alpha_1 \sin \alpha_2. \quad (9)$$

$J'$  and  $\delta'$  are the effective  $J$ -coupling constant and the effective offset when the irradiation is applied, respectively. The angles  $\alpha_1$  and  $\alpha_2$  in Eqs. 8 and 9 can be determined by the parameters  $\omega_1$ ,  $\delta$ , and  $J$  in the following equations:

$$\alpha_1 = \arctan(P - Q \tan \alpha_2) \quad (10)$$

$$\alpha_2 = \arctan\left(\frac{(P^2 - Q^2 + 1) - [(P^2 - Q^2 + 1)^2 + 4P^2 Q^2]^{1/2}}{2PQ}\right), \quad (11)$$

where

$$P = \omega_1 / \delta, \quad (12)$$

$$Q = J/2\delta. \quad (13)$$

We will not give too many details on the NMR signals calculations in this paper and only write down the results.

For the experiment in scheme (a),  $\rho(0) = S_x$ . The signal intensities in the numerical sequence starting from the left side in Fig. 2b are expressed as follows.

$$I_1(3Q) = I_9(F1Q) = \sin^4 \alpha_2, \quad (14)$$

$$I_2(\text{outside } SQ - 1) = I_8(\text{outside } SQ - 2) = \cos^4 \alpha_2, \quad (15)$$

$$I_3(DQ - 1) = I_4(DQ - 2) = I_6(ZQ - 1) = I_7(ZQ - 2) = 2\sin^2 \alpha_2 \cos^2 \alpha_2 \quad (16)$$

$$I_5(\text{central } SQ) = 2(\sin^4 \alpha_2 + \cos^4 \alpha_2). \quad (17)$$

Fig. 4 shows the signal intensities as functions of irradiation strength  $\omega_1$  with  $J = 187$  Hz,  $\delta = 100$  Hz for our experiments based on Eqs. 14-17. It is interesting to note that the MQ intensities increase with increasing irradiation strength in the weak region and soon reach their maxima

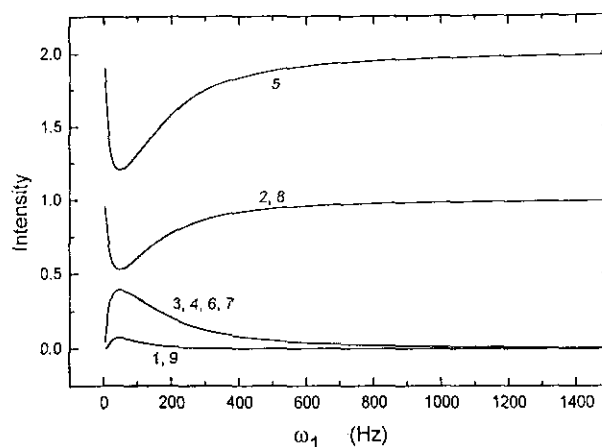


Fig. 4. Relative intensity of various possible transitions as a function of the irradiation field strength. These transitions are induced by a coherent state  $S_x$  under irradiation at the proton frequency in the  $\text{CH}_2$  group. The calculations are based on Eqs. 14-17 in the text.  $J = 187$  Hz,  $\delta = 100$  Hz. 1-3Q; 2, 8—the outside SQs; 3, 4—DQs; 5—the central SQ; 6, 7—ZQ; 9—F1Q. As the irradiation field increases the outside SQs merge with the central SQ and the intensity of the central peak increases by a factor of 2 as described in Fig. 2.

while the SQ intensities drop to their minima. When the irradiation strength is increased further, the MQ intensities will monotonously decrease while the SQ intensities increase. The MQs actually drop to zero intensity when the irradiation strength in frequency unit is about twice the  $J$  value while the SQs reach intensities that are the same as the ones without irradiation.

For the experiment in scheme (b),  $\rho(0) = 2I_2S_x$ . The signals can be expressed as follows.

$$I_1(3Q) = -I_9(F1Q) = -\sin\alpha_1\sin^3\alpha_2 \quad (18)$$

$$I_2(SQ-1) = -I_8(SQ-2) = -\cos\alpha_1\cos^3\alpha_2 \quad (19)$$

$$I_3(DQ-1) = -I_7(ZQ-2) \\ = -\sin\alpha_1\sin\alpha_2\cos^2\alpha_2 + \cos\alpha_1\sin^2\alpha_2\cos\alpha_2 \quad (20)$$

$$I_4(DQ-2) = -I_6(ZQ-1) \\ = -\sin\alpha_1\sin\alpha_2\cos^2\alpha_2 - \cos\alpha_1\sin^2\alpha_2\cos\alpha_2 \quad (21)$$

$$I_5(\text{central SQ}) = 0 \quad (22)$$

Fig. 5 shows the signal intensities as functions of the irradiation strength for the same system as in our experiment based on Eqs. 18-22. Here in the weak region, the MQ intensities initially increase with irradiation strength in a different manner compared to scheme(a). Besides, the 3Q and DQs intensities have a negative sign, as opposed to the ones for the F1Q and ZQs. In the meantime the absolute intensities of the two SQs drop quickly.  $I_1$ ,  $I_3$ ,  $I_7$ , and  $I_9$  reach their absolute maxima at about  $\omega_1 = J/4$ , while  $I_4$  and  $I_6$  at about  $\omega_1 = J$ .  $I_1$  and  $I_9$  monotonously decrease after reaching

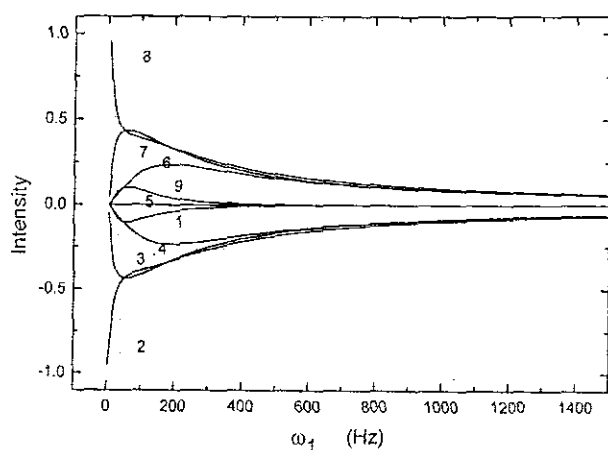


Fig. 5. The relative intensity of various possible transitions as a function of the irradiation field strength. These transitions are induced by a coherent state  $2I_2S_x$  under irradiation at the proton frequency in the  $\text{CH}_2$  group. The calculations are based on Eqs. 18-22 in the text.  $J = 187$  Hz,  $\delta = 100$  Hz. The numberings are the same as in Fig. 4.

their absolute maxima with increasing irradiation towards a decoupling situation. As shown in Fig. 5, when the irradiation strength in frequency unit reaches twice of the  $J$  value, all the absolute intensities vanish.

As one can see from Figs. 2 and 3, the two outside SQs in the  $\text{CH}_2$  group regularly merge with the central SQ when the irradiation strength  $\omega_1$  is increased. This decoupling process can be explicitly described by the effective coupling constant  $J'$  in Eq. 8. Fig. 6 shows  $J'$  of the  $\text{CH}_2$  spin system as a function of  $\omega_1$ .  $J'$  decreases monotonously and not linearly with increasing irradiation.

Figs. 4-5 have explicitly demonstrated the main phenomena shown in our experiments, at least qualitatively. However, the theoretical analysis is incomplete, e.g., the line broadening effect due to irradiation has been ignored. A quantitative comparison of the signal intensities in the experiments with the analysis is beyond the scope of this work. Nevertheless, the  $J'$  analysis does give a reasonable measurement in functional dependence on the irradiation field strength.

## CONCLUSION

In a heteronuclear spin system, a previously prepared SQ coherence of X-spin will introduce all the possible NMR signals, including SQs and MQs available in the system when irradiating the proton spins. These MQs appear in a relatively narrow range of irradiation strength, i.e., when  $\omega_1 < 2J$ . We have studied several samples, each containing only one of the  $\text{CH}$ ,  $\text{CH}_2$ , and  $\text{CH}_3$  groups, and conclude that this phenomenon is generally true. This study can also be devoted to the mechanism of Raman magnetic resonance.<sup>6-8</sup>

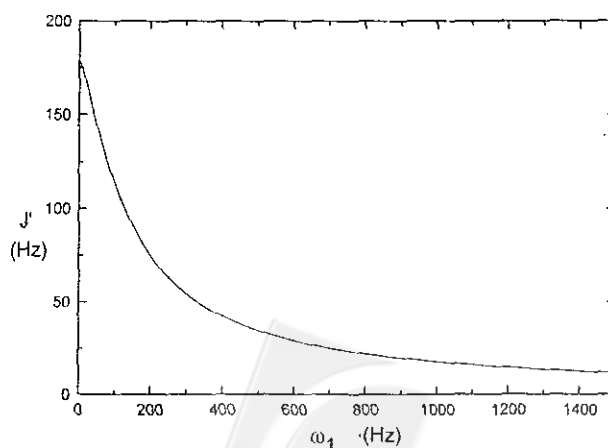


Fig. 6. The effective constant of spin coupling in  $\text{CH}_2$  as a function of the proton decoupling irradiation.



Care should be taken when the effective irradiation is not sufficient strong in a decoupling experiment, since the MQs can make the spectrum more complicated.

This experiment also demonstrates an easy approach to observe MQ signals in heteronuclear spin systems. A specific MQ signal can be selectively obtained when incorporating a MQ filter during the detection period, e.g., by inserting a pulsed gradient to the magnetic field. Besides, the reversed detection scheme,<sup>8</sup> i.e., observing proton signals while irradiating carbon spins, can also be adapted to conduct the experiments. No attempt is made here to mention all the possible experiments that exhibit this kind of phenomenon. However, it is believed that the phenomenon described in this article will enhance the understanding of Raman magnetic resonance experiments and the application of this phenomenon may be further explored. Studies following this line is under way.

#### ACKNOWLEDGMENT

CY is grateful to members of the IAMS for their kind hospitalities driving his sabbatical visit and to the National Science Council for a special research fellowship.

Received August 2, 1995.

#### Key Words

Spin decoupling; Multiple quantum NMR;  
Raman magnetic resonance.

#### REFERENCES

1. Bodenhausen, G. D. *Prog. Nucl. Magn. Reson. Spect.* **1981**, *14*, 137.
2. Weitekamp, D. *Adv. Magn. Reson.* **1983**, *11*, 111.
3. Munowitz, M.; Pines, A. *Adv. Chem. Phys.* **1987**, *66*, 1.
4. Royden, V. *Phys. Rev.* **1954**, *96*, 543.
5. Bloom, A. L.; Shoolery, J. N. *Phys. Rev.* **1955**, *97*, 1261.
6. Yang, D.; Ye, C. *Chem. Phys. Lett.* **1990**, *173*, 216.
7. Yang, D.; Ye, C. *Sci. China* **1992**, *35A*, 842.
8. Yang, D.; Ye, C. *J. Magn. Reson.* **1992**, *97*, 271.
9. Freeman, R.; Anderson, W. A. *J. Chem. Phys.* **1962**, *37*, 2053.
10. Morris, G. A.; Freeman, R. *JACS* **1979**, *101*, 760.
11. Anderson, W. A. *Phys. Rev.* **1956**, *104*, 850.
12. Kaplan, J. I.; Meiboom, S. *Phys. Rev.* **1957**, *106*, 499.
13. Miao, X.; Ye, C. *Kexue Tongbao (Chi. Sci. Bull.)* **1994**, *39*, 1939.

